



Raman investigation and functional characterization of $(\text{Pb}_{0.8}\text{La}_{0.2})(\text{Mg}_{0.4}\text{Nb}_{0.6})\text{O}_3$ ceramics prepared by the columbite method

A. Ianculescu^a, M.M. Carnasciali^b, L.P. Curecheriu^{c,*}, L. Mitoseriu^c

^a Polytechnics University of Bucharest, 1-7 Gh. Polizu, P.O. Box 12-134, 011061 Bucharest, Romania

^b Dept. of Chemistry and Industrial Chemistry, University of Genoa, 31 Via Dodecaneso, Genoa I-16146, Italy

^c Department of Solid State and Theoretical Physics, Al. I. Cuza University, Bv. Carol 11, 700506 Iasi, Romania

ARTICLE INFO

Article history:

Received 28 May 2010

Received in revised form 7 August 2010

Accepted 16 August 2010

Available online 27 August 2010

Keywords:

Microstructure–final

Raman spectroscopy

Dielectric properties

Niobates

Perovskites

ABSTRACT

$(\text{Pb}_{0.8}\text{La}_{0.2})(\text{Mg}_{0.4}\text{Nb}_{0.6})\text{O}_3$ relaxor ceramics have been prepared by columbite method by using (i) MgO and (ii) $(\text{MgCO}_3)_4 \cdot \text{Mg}(\text{OH})_2 \cdot 4\text{H}_2\text{O}$ precursors (denoted as PLMN1 and PLMN2 respectively). The dielectric data show relaxor behaviour in the frequency range of 10 Hz to 1 MHz, with dielectric constant values in the range of 310–350 for PLMN1 and 240–260 for PLMN2 and a permittivity maxima at the temperature $T_m = 179$ K and $T_m = 174$ K, respectively (for $f = 1$ MHz). The Raman spectra proved the stability of the nanopolar order far above T_m , as observed in many Pb-based relaxors. This is demonstrated by the existence of some modes (at ~ 300 , 500 and 780 cm^{-1}) up to around 773 K. Anomalies of some Raman modes (integrated intensity and FWHM) have been found in the range of T_m , proving the phase transition from pseudo-cubic relaxor to cubic paraelectric state, where the stability of the vibration modes is affected by the fluctuations associated to the phase transitions.

© 2010 Elsevier B.V. All rights reserved.

1. Introduction

Among the lead-based relaxor ferroelectric materials of general formula $\text{Pb}(\text{B}'\text{B}'')\text{O}_3$, those derived from lead magnesium niobate, $\text{Pb}(\text{Mg}_{1/3}\text{Nb}_{2/3})\text{O}_3$ (PMN) are probably the most widely studied one because of its excellent dielectric and electrostrictive properties [1]. However, a significant problem concerning PMN-based ceramics is the difficulty in preparing a single-phase material of only perovskite structure without the appearance of a pyrochlore phase that can be detrimental to the dielectric properties [2–4]. In order to overcome this disadvantage, various synthesis techniques for suppressing the formation of pyrochlore-type compound (i.e. columbite method [4–6] and mechanical activated synthesis [5–7]) have been reported in the literature.

Although former studies [8,9] showed that the degree of ordering and the size of the ordered domains can be enhanced by incorporating lanthanum into lead magnesium niobate lattice [10–14], however there are only a few papers concerning the lanthanum influence on the relaxor behaviour of the PLMN ceramics [8,15].

The aim of this work is to investigate the influence of the magnesium source on the Raman characteristics, microstructure and

dielectric behaviour of the $\text{Pb}_{0.8}\text{La}_{0.2}\text{Mg}_{1.3}\text{Nb}_{2/3}\text{O}_3$ ceramics prepared via columbite route.

2. Experimental

2.1. Sample preparation

The starting materials were reagent-grade PbO (Fluka), MgO (Merck), $(\text{MgCO}_3)_4 \cdot \text{Mg}(\text{OH})_2 \cdot 5\text{H}_2\text{O}$ (Carlo Erba) and Nb_2O_5 (Johnson Matthey Chemicals Ltd.) powders.

The samples prepared for this study were the lanthanum-modified lead magnesium niobate ceramics described by the formula $\text{Pb}_{0.8}\text{La}_{0.2}\text{Mg}_{0.4}\text{Nb}_{0.6}\text{O}_3$ and obtained by using two different magnesium precursors: (a) magnesium oxide (PLMN1) and magnesium basic carbonate (PLMN2), respectively. Synthesis of the PLMN samples was carried out by the columbite method proposed by Swartz and Shrout [16]. Thus, in the first stage, MgO and Nb_2O_5 powders were prereacted at 1000°C in air to form the nonstoichiometric columbite. In order to obtain La-modified lead magnesium niobate, in the second stage appropriate amounts of PbO and La_2O_3 were added to the nonstoichiometric columbite powders derived from the both magnesium precursors. The details of the preparation, as well as the succession of the chemical reaction were reported elsewhere [17]. The calcined powders with polyvinyl alcohol (PVA) added as binder, were pressed into pellets of 10 mm diameter and ~ 3 mm thickness, which were then sintered for 4 h in air at 1200°C . Sintering was performed inside closed platinum crucibles and the pellets were covered with powders of the same composition to minimize the lead loss during the thermal treatments.

2.2. Sample characterization

The microstructure of the ceramics was investigated by scanning electron microscopy (SEM) using JEOL JSM-6400 and Hitachi S2600N equipments. The sinterability of the PLMN ceramics was estimated by means of the values of the relative density calculated as ratio between the apparent density determined by

* Corresponding author. Tel.: +40 232 201175; fax: +40 232 201205.

E-mail addresses: a.ianculescu@rdslink.ro (A. Ianculescu), lavinia.curecheriu@stoner.phys.uaic.ro (L.P. Curecheriu).

the hydrostatic method and the theoretical density determined from the XRD data (reported elsewhere [15,17]).

The phase composition of the sintered samples was studied by X-ray diffraction (XRD) with a Brucker-AXS D8 diffractometer, using Ni-filtered Cu K α radiation ($\lambda = 1.5418 \text{ \AA}$), a scan step of 0.02° and a counting time of 1 s/step in the 2θ range of $15\text{--}90^\circ$.

For the electric measurements, Ag–Pb electrodes were deposited on the plane-parallel polished surfaces of the ceramics followed by annealing in air at 500°C for 12 h. The dielectric measurements were performed with an impedance analyzer Solartron SI1260 for temperatures of $80\text{--}250 \text{ K}$ with a heating/cooling rate of 0.5 K/min in the frequency range $10\text{--}10^6 \text{ Hz}$.

The Raman spectra were recorded in back scattering geometry by using a RENISHAW RM2000 micro-Raman spectrometer with 785 nm radiation, $2 \text{ }\mu\text{m}$ spot diameter and $10 \text{ }\mu\text{m}$ field depth in the temperature range ($100, 670 \text{ K}$), by using LINKAM thermal cells. Due to the instrumental cutoff, soft modes with wave numbers lower than 80 cm^{-1} cannot be observed. All the spectra obtained in various microregions of the samples are similar and well reproducible in time, indicating a high homogeneity of all the present samples at micrometric level.

3. Results and discussions

SEM investigations on the surface of the both PLMN sample sintered at $1200^\circ\text{C}/4 \text{ h}$ pointed out a relative homogenous, fine-grained (average grain size of $\sim 3.5 \text{ }\mu\text{m}$) microstructure (Fig. 1(a) and (b)). Unlike the PLMN2 sample derived from magnesium basic carbonate, which presents a more porous microstructure and not well-defined grain boundaries (Fig. 1(b)), a better densification,

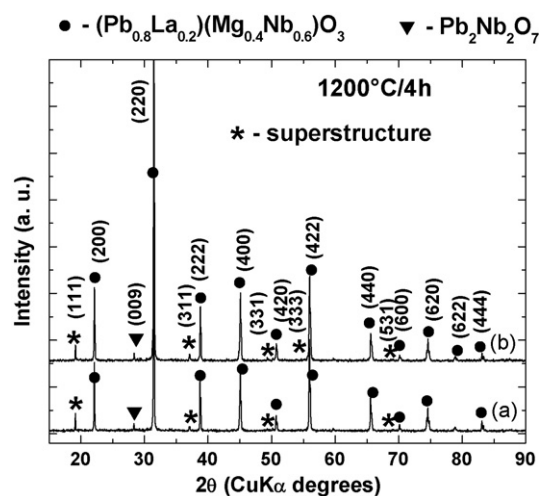


Fig. 2. Room temperature X-ray diffraction pattern of the samples sintered at $1200^\circ\text{C}/4 \text{ h}$: (a) PLMN1 and (b) PLMN2.

involving a lower amount of intergranular porosity and perfect triple junctions between the grains was noticed for the sample PLMN2 derived from MgO precursor (Fig. 1(a)).

The X-ray diffraction patterns of the PLMN1 and PLMN2 sample sintered at $1200^\circ\text{C}/2 \text{ h}$ are very similar, showing the presence of the well crystallized PLMN perovskite as a major phase and small amounts of a secondary $\text{Pb}_2\text{Nb}_2\text{O}_7$ pyrochlore phase, identified at the detection limit. The supplementary $(1\ 1\ 1)$, $(3\ 1\ 1)$, $(3\ 3\ 1)$ and $(5\ 3\ 1)$ diffraction peaks indicate the formation of the 1:1 short range ordering induced by the La addition (Fig. 2).

Unlike the non-modified PMN ceramics which exhibit high dielectric constant values ($12,000\text{--}13,500$) at T_m for $f = 10 \text{ Hz}$ [18], the presence of La causes a strong reduction of the real part of the dielectric permittivity, as well as a visible flattening of the $\epsilon'(T)$ characteristic. The decrease of the dielectric constant ϵ' can be explained in terms of the large porosity (15% for PLMN1 and 26% for PLMN2) of our ceramics and also because of the positive charge provided by La, facilitating the growth of 1:1 chemically ordered regions, which most probably are not ferroelectric in nature [12] (Fig. 3(a) and (b)). Another cause of the real permittivity decrease may be related to the microstructural features (small grain size and porosity). In spite of the $\epsilon'(T)$ flattening, the relaxor behaviour (dispersion of the dielectric constant values against the frequency at $T < T_m$) was still clearly observed for both PLMN ceramics (Fig. 3(a)). T_m values are ranged between 155 and 179 K for frequencies ranged between 10 Hz and 1 MHz and they are almost similar for PLMN1 and PLMN2, indicating that the Mg precursor type has no influence on the relaxor behaviour. However, the higher values of the dielectric constant obtained for the PLMN1 ceramic in all the frequency range analyzed may be due to the better densification of this sample ($\rho_r = 85.09\%$) comparing to that one of PLMN2 ($\rho_r = 74.07\%$). Thus, at T_m of 155 K (for $f = 10 \text{ Hz}$), dielectric constants of 355 and 265 were recorded for PLMN1 and PLMN2, respectively.

In spite of lower density, low values of dielectric losses ($\tan \delta < 3\%$) have been obtained in the investigated temperature range for both PLMN samples sintered at $1200^\circ\text{C}/4 \text{ h}$. The temperature dependence of reciprocal dielectric constant at different frequency is shown in Fig. 3b. The temperature where $\epsilon^{-1}(T)$ starts to deviate from Curie–Weiss law, is considered the onset temperature of local polarization is affected by a high degree of uncertainty. The Cole–Cole diagram shows a single component in the frequency range under investigation, indicating the lack of the grain-boundary phenomena.

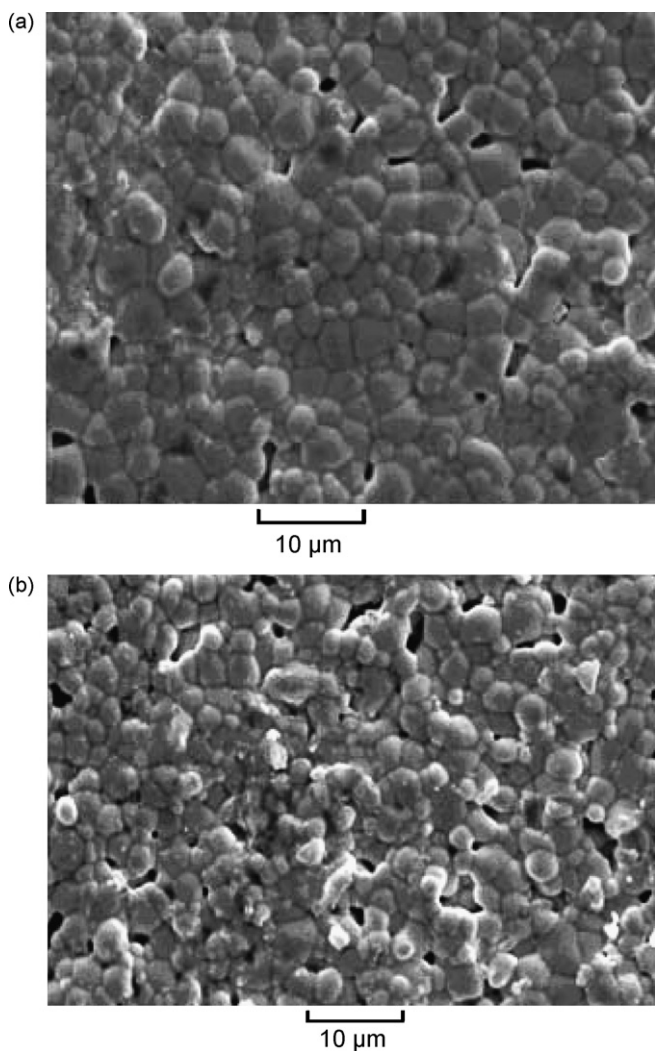


Fig. 1. SEM images of the samples sintered at $1200^\circ\text{C}/4 \text{ h}$: (a) PLMN1 and (b) PLMN2.

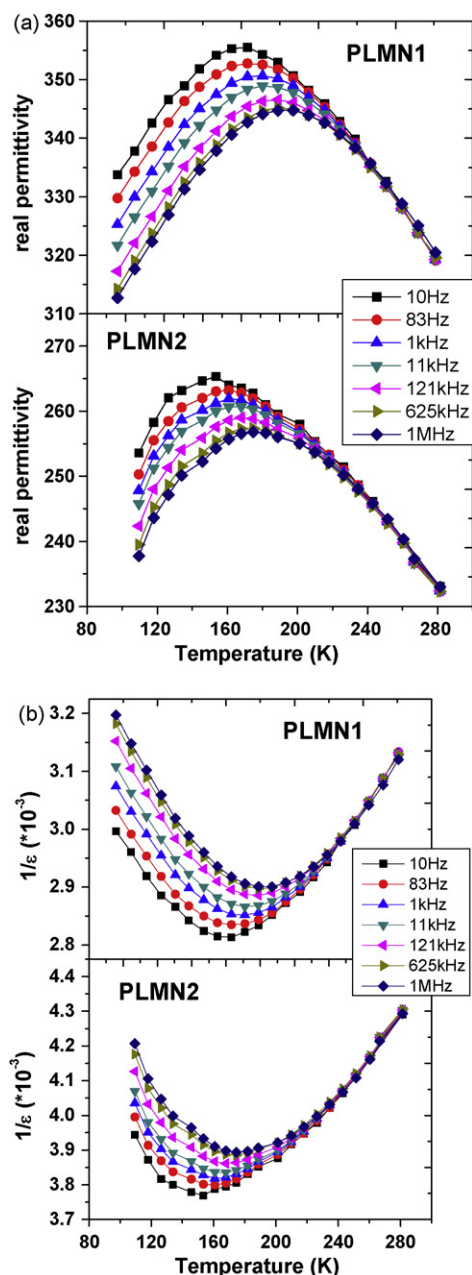


Fig. 3. Temperature dependence of (a) real part of permittivity for PLMN1 and PLMN2 various frequencies and (b) reciprocal dielectric constant for both ceramics.

The empirical Vogel–Fulcher law [19] were used to characterize the frequency dispersion of T_m of PLMN1:

$$f = f_0 \exp \left[-\frac{E_a}{k(T_m - T_{VF})} \right], \quad (1)$$

where f is the measurement frequency and E_a , T_{VF} and f_0 are the parameters. In relaxors, T_{VF} is named freezing temperature of dynamics of polar nanoregions due to cooperative interactions between their moments. Fig. 4 shows the logarithm of measurement frequency vs. T_m and the fit with V-F parameters. From fit of T_m we determine $E_a = 0.067$ eV, $f_0 = 3.26 \times 10^{12}$ Hz and $T_{VF} = 132$ K.

The Raman spectra of the two types of PLMN ceramics show very similar features (Fig. 5). The Raman spectra were analyzed using damped-harmonic-oscillator model, wherefrom oscillator strength can be determined by Raman mode. With the exception of the main mode denoted as (1), all the Raman bands are broad and some bands

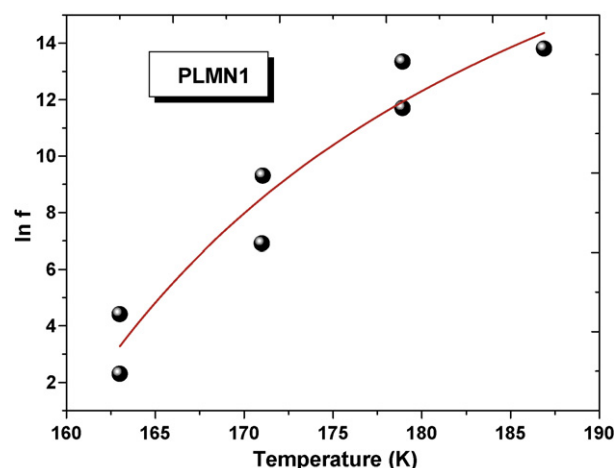


Fig. 4. Natural logarithm of frequency vs. temperature for PLMN1. Solid curves represent the fitting to the Vogel–Fulcher law of Eq. (1).

are overlapped (Fig. 5). The Raman bands can be analyzed using a two-phase model, in which 1:1 B-site ordered nanoregions with space group $Fm\bar{3}m$ ($Z=2$) are dispersed in a disordered matrix with an average space group of $Pm\bar{3}m$ ($Z=1$) [20,21]. For $Pm\bar{3}m$, there is no Raman active mode, whereas for $Fm\bar{3}m$ there are Raman active modes according to the group theoretical analysis [22]. The most significant band in Fig. 5 is the mode around 780 cm^{-1} (A_{1g} mode, denoted as (1) in the present paper), associated to the motion of the oxygen atoms like the breathe type of a free octahedron. This mode was interpreted as related to the ordered nanopolar regions of space group $Fm\bar{3}m$ and thus considered as a probe for the degree of 1:1 chemical order at the B site in the Pb-based relaxors [20]. The position of this mode is not sensitive to the small microstructural differences present in the two types of PLMN ceramics prepared by two Mg precursors (as demonstrated by Fig. 5) and its position is very stable against the temperature variations (Figs. 6 and 7). The evolution with temperature of the position of all the other modes shows a general tendency of softening with increasing temperature (Fig. 7). A reducing intensity of all the modes and a continuous increasing of the full width at half maximum (FWHM) with increasing temperature were also observed (as shown in Fig. 8, where the temperature dependence of the FWHM of the peak 1 in PLMN1 and PLMN2 is presented).

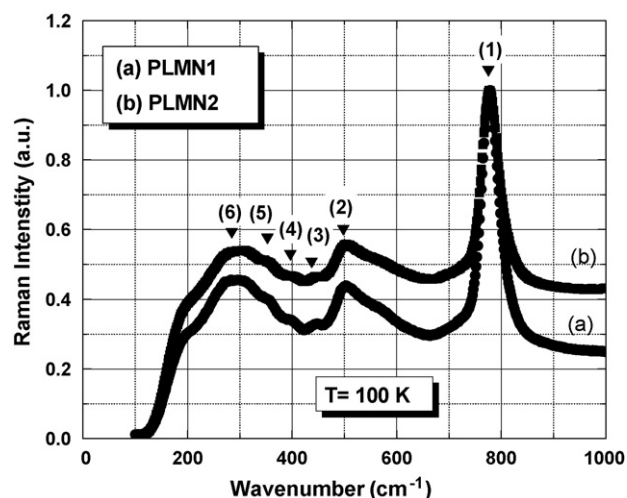


Fig. 5. Raman spectra recorded at $T = 100$ K for PLMN1 and PLMN2, respectively.

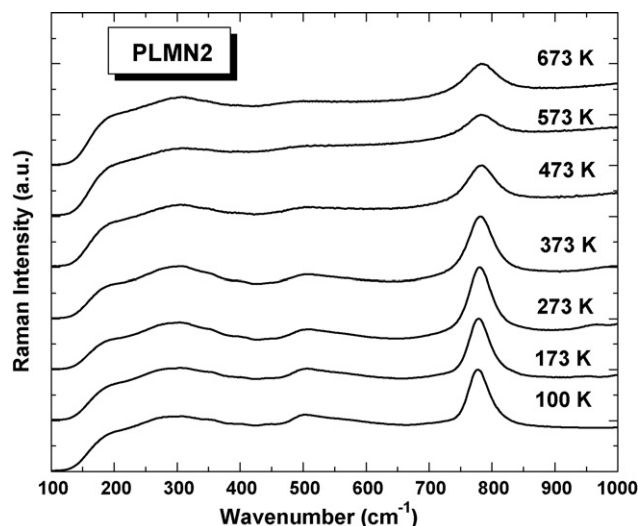


Fig. 6. Temperature dependence of the Raman spectrum for PLMN2 sample.

As demonstrated by the dielectric data [15], a frequency-dependent maximum of the permittivity was located in the range of temperatures of $T_m \in (133, 183)$ K for $f \in (10, 10^6)$ Hz. As for all the relaxors characterized by a diffuse phase transition, a large temperature range is necessary for the ferroelectric relaxor-paraelectric state transition. In any case, it was found that above the room temperature, both the PLMN ceramics are in their paraelectric state. The fact that the mode (1) still exists far above the range of T_m and it did not disappear even at 673 K (Fig. 5) demonstrates that the 1:1 B-site ordered nanoregions are very stable against the thermal fluctuations and persist many hundred degrees above the temperature corresponding to the maximum permittivity.

As observed in Fig. 9, the intensity of the main mode (1) has an anomalous variation with temperature, with a pronounced minimum in the range of (113, 183) K, which corresponds to the range of the dielectric anomaly. The observed behaviour is an indication of the fluctuations of the local order (reflected in the Raman spectra) that take place during the transition relaxor-paraelectric in a large range of temperatures. Even this transition separates very similar macroscopic states and it is not accompanied by obvious changes in the crystalline structure (pseudo-cubic and cubic phases), rearrangements of the nanopolar domains in metastable states cause a

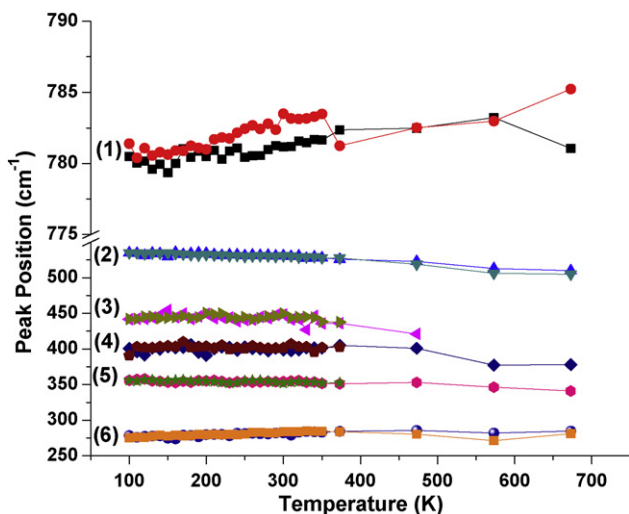


Fig. 7. Position of the characteristic Raman peaks versus the temperature for the PLMN1 and PLMN2 samples.

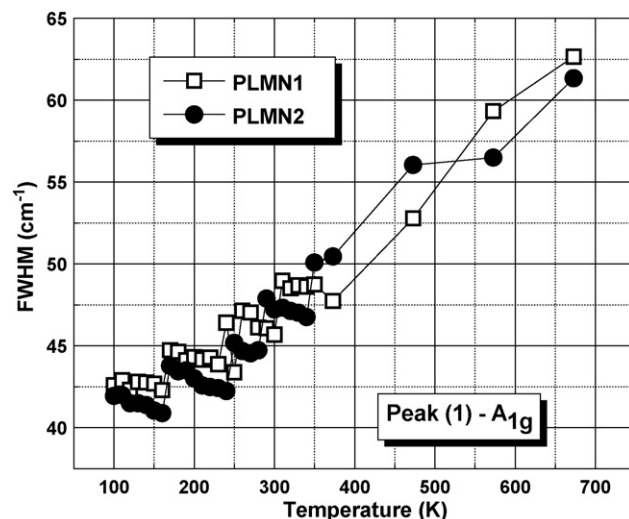


Fig. 8. Variation of the Raman FWHM (full width at half maximum) against the temperature for the main A_{1g} peak (denoted as peak (1)) in PLMN1 and PLMN2, respectively.

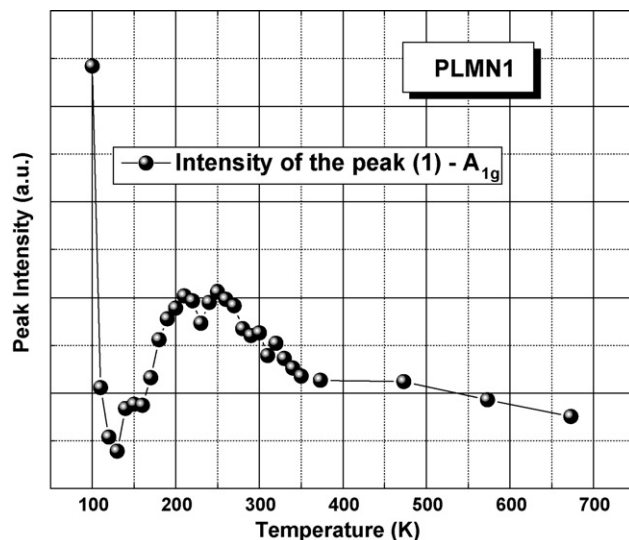


Fig. 9. Variation of the integrated Raman intensity against the temperature for the main A_{1g} peak in PLMN1.

maximum value of the permittivity in the Curie range and produce fluctuations of the local ordering that can be probed by Raman scattering. These anomalies are related both to the changes of the force constant that give rise to anomalies of the Raman shift of some bands and also to the fluctuations of the states population that cause anomalies in the intensity of some peaks. Similar changes in the intensity of some Raman bands at phase transitions were observed in many relaxors [23–25].

4. Conclusion

$(\text{Pb}_{0.8}\text{La}_{0.2})(\text{Mg}_{0.4}\text{Nb}_{0.6})\text{O}_3$ relaxor ceramics have been prepared by columbite method by using (i) MgO and (ii) $(\text{MgCO}_3)_4 \cdot \text{Mg}(\text{OH})_2 \cdot 4\text{H}_2\text{O}$ precursors (denoted as PLMN1 and PLMN2, respectively).

The type of the magnesium precursor seems to have no significant effect on the phase composition, but obviously influenced the densification, as well as the dielectric constant values for the PLMN samples.

The dielectric data show relaxor behaviour in the frequency range of 10 Hz to 1 MHz, with permittivity values in the range of (310–355) for PLMN1 derived from MgO precursor and 240–265 for PLMN2 derived from magnesium basic carbonate precursor. These data are in accord with the SEM investigations, which indicated a better densification of the PLMN1 sample in comparison with PLMN2. However, the type of the Mg precursor seems to have not a significant influence on the value of the temperature of the permittivity maximum, especially at lower frequency ($T_m = 155\text{K}$ at $f = 1\text{ kHz}$ for both PLMN sample).

The Raman spectra proved the stability of the nanopolar order far above T_m , as observed in many Pb-based relaxors. This is demonstrated by the existence of some modes (at ~ 300 , 500 and 780 cm^{-1}) up to around 673. Anomalies of some Raman modes (integrated intensity and full width at half maximum – FWHM) have been found in the range of T_m , proving the phase transition from pseudo-cubic relaxor to cubic paraelectric state, where the stability of the vibration modes is affected by the fluctuations associated to the phase transitions.

Acknowledgement

L.C. acknowledges financial support from POSDRU 89/1.5/S/49944.

References

- [1] S.L. Swartz, T.R. Shrout, W.A. Schulze, L.E. Cross, *J. Am. Ceram. Soc.* 67 (1984) 311–315.
- [2] T.R. Shrout, A. Halliyal, *Am. Ceram. Soc. Bull.* 66 (1987) 704–711.
- [3] D.H. Kang, K.H. Yoon, *Ferroelectrics* 87 (1988) 255–264.
- [4] A.L. Costa, C. Galassi, G. Fabri, E. Roncari, C. Capianni, *J. Eur. Ceram. Soc.* 21 (2001) 1165–1170.
- [5] J. Wang, X. Junmin, W. Dongmei, N. Weibeng, *Solid State Ionics* 124 (1999) 271–279.
- [6] J. Wang, X. Junmin, W. Dongmei, N. Weibeng, *J. Am. Ceram. Soc.* 82 (1999) 1358–1360.
- [7] X. Junmin, J. Wang, T.M. Rao, *J. Am. Ceram. Soc.* 84 (2001) 660–662.
- [8] J. Chen, H.M. Chan, M.P. Harmer, Ordering Structure, *J. Am. Ceram. Soc.* 72 (1989) 593–598.
- [9] Z. Xu, S.M. Gupta, D. Viehland, *J. Am. Ceram. Soc.* 83 (2000) 181–188.
- [10] L.-J. Lin, T.-B. Wu, *J. Am. Ceram. Soc.* 73 (1990) 1253–1256.
- [11] L.-J. Lin, T.-B. Wu, *J. Am. Ceram. Soc.* 74 (1991) 1360–1363.
- [12] D.M. Fanning, I.K. Robinson, S.T. Jung, E.V. Colla, D.D. Viehland, D.A. Payne, *J. Appl. Phys.* 87 (2000) 840–848.
- [13] K. Park, L. Salamanca-Riba, M. Wuttig, D. Viehland, *J. Mater. Sci.* 29 (1994) 1284–1289.
- [14] X. Pan, W.D. Kaplan, M. Rühle, *J. Am. Ceram. Soc.* 81 (1998) 597–605.
- [15] A. Ianculescu, A. Brăileanu, M. Viviani, L. Mitoşeriu, *J. Eur. Ceram. Soc.* 27 (2007) 4375–4378.
- [16] S.L. Swartz, T.R. Shrout, *Mater. Res. Bull.* 17 (1982) 1245–1250.
- [17] A. Ianculescu, A. Brăileanu, I. Pasuk, C. Popescu, *J. Therm. Anal. Calorim.* 80 (2005) 663–670.
- [18] L. Mitoşeriu, A. Ianculescu, M.M. Carnasciali, A. Brăileanu, L. Curecheriu, *Ferroelectrics* 369 (2008) 157–169.
- [19] A.E. Glazounov, A.K. Tagantsev, *Appl. Phys. Lett.* 73 (1998) 856.
- [20] F. Jiang, S. Kojima, C. Zhao, C. Feng, *J. Appl. Phys.* 88 (2000) 3608–3612.
- [21] F. Jiang, S. Kojima, C. Zhao, C. Feng, *Appl. Phys. Lett.* 79 (2001) 3938–3940.
- [22] I.G. Siny, S.G. Lushnikov, R.S. Katiyar, V.H. Schmidt, *Ferroelectrics* 226 (1999) 191–215.
- [23] S. Gupta, R.S. Katiyar, R. Guo, A.S. Bhalla, *J. Raman Spectrosc.* 31 (2000) 921–924.
- [24] S. Kim, I.S. Yang, J.K. Lee, K.S. Hong, *Phys. Rev. B* 64 (2001) 094105.
- [25] L. Mitoşeriu, M.M. Carnasciali, P. Piaggio, P. Nanni, *J. Appl. Phys.* 96 (2004) 4378–4385.